

Underwater Optical Ranging: A Hybrid LIDAR-RADAR Approach

Dennis L. Waldron III
 Dr. Linda Mullen, Advising
 Lafayette College
 NAVAIR

I. BACKGROUND

Proximity detection underwater is performed primarily by sending and receiving some form of magnetic or acoustic radiation. This is done by propagating a known output signal, and measuring the response of or disturbance from some target. However, these systems have limitations in how much range resolution and accuracy they can provide under certain conditions.

Recognizing this short-coming, optical techniques for underwater ranging are being investigated. Optical systems can provide update rates on the order of mega-Hertz because it depends on the speed of light instead of the speed of sound. Perhaps most importantly, they can provide much greater resolution and accuracy in their measurements than existing systems, theoretically on the order of centimeters, or even sub-centimeter, depending on the configuration. There is, in fact, a US Navy requirement for a high-precision, large dynamic-range, proximity detector that is as insensitive as possible to changing water conditions, with a range of less than two meters.

However, when traveling through a medium such as water, an optical signal will attenuate exponentially because of absorption and scattering. The absorption coefficient, or a , characterizes the photons that are extinguished and cannot be recovered by the detector. Physically, when dealing with wavelengths in the blue to IR spectrum (about 400nm to 100 μ m), this loss is caused by the photons interacting with the water molecules and some particulates in the water. Wavelengths in the near infrared (NIR) spectrum interact more strongly, and absorb more quickly [1]. Running out of signal due to absorption is called reaching your photon limit. An analogy would be like driving a car on a clear night- if the vehicle's high beams are turned on, the driver can see farther. In other words, sending more photons into the environment (i.e. using a greater optical power), will allow the system better range when this type of loss is dominant.

Scattering, characterized by the scattering coefficient, b , causes a photon to be deflected from its trajectory rather than simply being absorbed. This kind of loss comes from photons bouncing off of various particulates in the water, both organic and inorganic; the more turbid the water is, the more prone photons are to scatter [1]. A small percentage of photons have an angle of reflection large enough to become "backscatter." These photons are reflected back at the detector without making it to the target and are especially troublesome; they become noise, carrying no useful information. Reaching a point where the return signal is dominated by this backscatter noise is referred to as reaching the backscatter limit. Returning to the night-driving analogy, this type of loss would be like the driver turning on high beams in a fog- the driver might be able to see a little farther if the fog is light enough, but eventually he or she would just be blinded by the reflected light.

These two measures of signal loss are often combined additively into a single measure, called the beam attenuation coefficient, or c . This is the total loss in signal strength. The challenge in performing optical proximity detection in the underwater environment is to receive more photons from the underwater object than either the receiver noise floor or the ambient environment. In the next section, two different approaches for underwater optical proximity detection will be discussed.

II. DESIGN OF AN UNDERWATER OPTICAL RANGING SYSTEM

A. Previous Design

Fig. 1 shows a previous approach to an optical ranging system. A light source is set next to a receiver such that the cone of light emitted can be seen within the field of view (FOV) of the receiver when it is reflected off of a target. As the target gets closer, the amount of light received gets greater, and the signal amplitude increases. However, as the target is moved closer still, the common volume of the cone of light and the FOV gets smaller, causing the amplitude to fall off. Distance can then be determined relative to the peak amplitude observed [2].

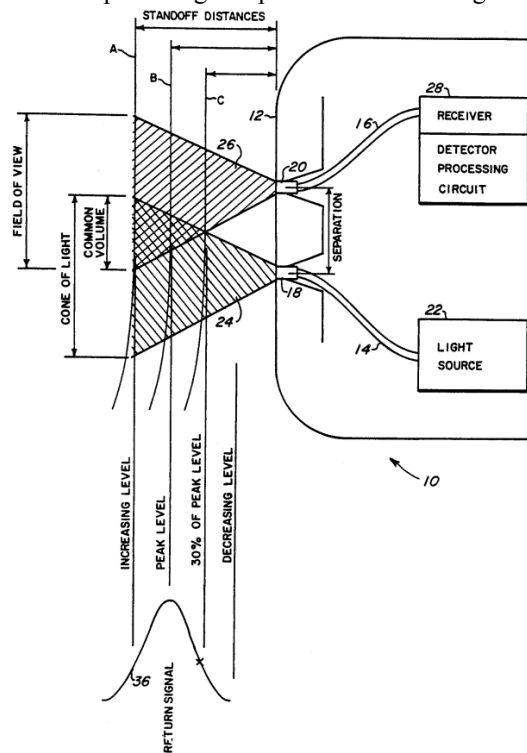


Fig. 1 A previous approach to optical ranging underwater using return signal amplitude [2].

Report Documentation Page

Form Approved
OMB No. 0704-0188

Public reporting burden for the collection of information is estimated to average 1 hour per response, including the time for reviewing instructions, searching existing data sources, gathering and maintaining the data needed, and completing and reviewing the collection of information. Send comments regarding this burden estimate or any other aspect of this collection of information, including suggestions for reducing this burden, to Washington Headquarters Services, Directorate for Information Operations and Reports, 1215 Jefferson Davis Highway, Suite 1204, Arlington VA 22202-4302. Respondents should be aware that notwithstanding any other provision of law, no person shall be subject to a penalty for failing to comply with a collection of information if it does not display a currently valid OMB control number.

1. REPORT DATE JUN 2010		2. REPORT TYPE N/A		3. DATES COVERED -	
4. TITLE AND SUBTITLE Underwater Optical Ranging: A Hybrid LIDAR-RADAR Approach				5a. CONTRACT NUMBER	
				5b. GRANT NUMBER	
				5c. PROGRAM ELEMENT NUMBER	
6. AUTHOR(S)				5d. PROJECT NUMBER	
				5e. TASK NUMBER	
				5f. WORK UNIT NUMBER	
7. PERFORMING ORGANIZATION NAME(S) AND ADDRESS(ES) Lafayette College NAVAIR				8. PERFORMING ORGANIZATION REPORT NUMBER	
9. SPONSORING/MONITORING AGENCY NAME(S) AND ADDRESS(ES)				10. SPONSOR/MONITOR'S ACRONYM(S)	
				11. SPONSOR/MONITOR'S REPORT NUMBER(S)	
12. DISTRIBUTION/AVAILABILITY STATEMENT Approved for public release, distribution unlimited					
13. SUPPLEMENTARY NOTES See also ADM202806. Proceedings of the Oceans 2009 MTS/IEEE Conference held in Biloxi, Mississippi on 26-29 October 2009. U.S. Government or Federal Purpose Rights License., The original document contains color images.					
14. ABSTRACT					
15. SUBJECT TERMS					
16. SECURITY CLASSIFICATION OF:			17. LIMITATION OF ABSTRACT SAR	18. NUMBER OF PAGES 7	19a. NAME OF RESPONSIBLE PERSON
a. REPORT unclassified	b. ABSTRACT unclassified	c. THIS PAGE unclassified			

While such a system is elegant in its simplicity and relatively compact, it is an extremely limited approach to ranging, as it is only able to operate over short distances, on the order of a few centimeters. In addition, a large amount of optical power is needed to operate such a system, especially if one wishes to increase the operating range. Practically, these factors limit the applications and usefulness of such a system.

B. A Hybrid Approach

A natural choice for precision ranging is coherent LIDAR (Light Detection and Ranging). However, it cannot be used directly in water because environmental effects cause a loss of optical coherence. On the other hand, RADAR (Radio Detection and Ranging) offers coherent detection, but since microwaves attenuate so rapidly in water, they cannot propagate. A solution is to modulate a light signal with a microwave signal, thus forming a hybrid approach. Using this hybrid signal, we are able to take advantage of the coherent detection of the RF modulation envelope, the RADAR signal, to measure range to a target.

Using this hybrid approach has previously been demonstrated by researchers at NAVAIR’s Patuxent River, Maryland facility to improve the performance of underwater imaging systems allowing for a range of greater than ten meters [3]. This system used a wavelength in the blue-green spectral region (450 to 550nm) due to the absorption characteristics of pure water, as seen in Fig. 2. However, since the optical proximity detector is being developed for a shorter range, less than two meters, other wavelengths are being considered. By choosing a higher wavelength in the red to NIR region (660 to 830nm in our case), optical loss will be dominated by absorption. This means that the effect of scattering on measurement accuracy is limited. And, since scattering is dictated by water turbidity, a change in water turbidity will not have as much of an effect on the measurement. Thus, the system will be able to operate more reliably in a number of environments. Laser diodes that can be modulated at megahertz rates are also readily available at these wavelengths, which is beneficial for making the system compact and efficient.

III. EXPERIMENTAL SETUP

A. Laser

Traveling the path of the signal through our experimental setup, seen in Fig. 3, we start with the laser. In our experiments, we tested three wavelengths: NIR, 830nm; red, 660nm; and green, 532nm. We used green as a basis of comparison, since we have used this wavelength extensively in the past.

All were continuous wave (CW) lasers. The NIR laser was a laser diode modulated via current injection with an average optical output power of about 50mW when modulated at 66MHz. The red laser was likewise a laser diode, this one with an average output power of about 10mW at 70MHz. The green was a solid state laser with an average output power on the order of a few watts, of which we only used a maximum of about 200mW. We used an external electro-optic (EO) modulator to achieve 70MHz modulation (the EO modulator and the necessary RF amplifier are not shown in the Fig. 3). In all cases, the laser was driven by the same RF generator as was the demodulator.

B. Target

Following the signal path, we come to the target. It was placed in a windowed water tank, 3.7m long and 1m tall and wide. It was suspended from an optical rail 2.5m long which was itself mounted over the tank so that the target distance could be easily varied. The target was 46cm wide and 30cm tall, and had a matte surface. We assumed this surface to be perfectly diffuse. In order to see the effects of target “strength,” the target was split vertically down the center. One side was then painted black, and the other painted a light grey so that

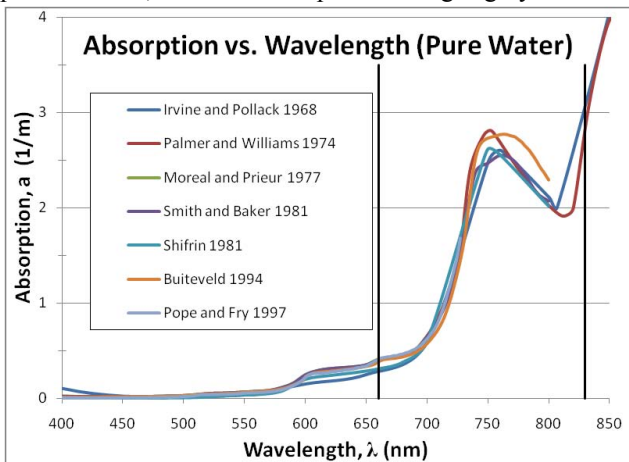


Fig. 2 Various data sets showing the effects of wavelength on absorption. Absorption is greater in the near IR region (800nm-1µm) compared to the visible (400-700nm). [4] [5] [6] [7] [8] [9] [10]

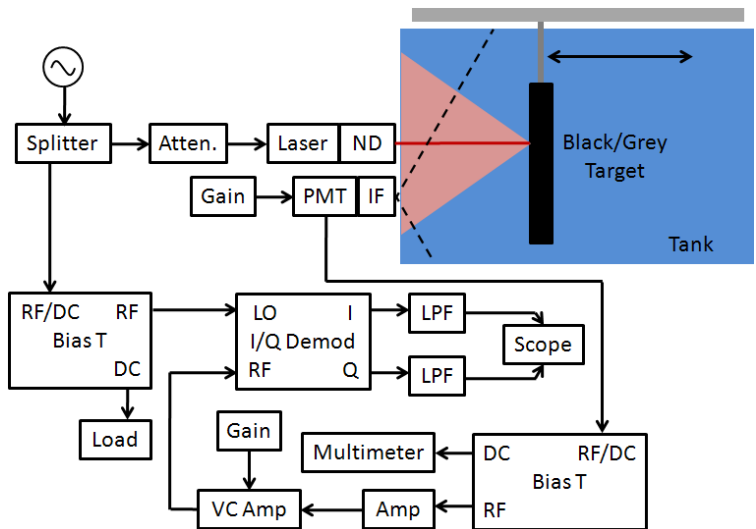


Fig. 3 A system block diagram. The dotted black lines from the PMT/ Filter assembly are a sample field of view. The red line from the laser/ ND assembly represents the beam. The lighter red is a diffuse reflection from the target.

they had different reflectivities. The target could then be positioned so that only one side or the other was being used at a time.

C. Detector

For our detector, we used a red enhanced photo-multiplier tube (PMT) with an 8mm aperture. A PMT was ideal because we did not need a large detector bandwidth, but we did need a relatively large detector surface area and moderately sized FOV. A PMT was also ideal for very low light levels, offering a gain of up to 10^6 . The gain of the PMT was set via a simple voltage divider circuit to the recommended maximum gain. Even being red-enhanced, the quantum efficiency at NIR wavelengths was much lower than at other wavelengths in the visible region, resulting in about two orders of magnitude less anode sensitivity [11].

An interference filter (IF) with a bandwidth of 10nm centered at 660 or 830nm was used for red and NIR, respectively. For the green, we used an IF centered at 532nm with a bandwidth of 5nm, as it was readily available in our lab. Additionally, the IF had the ancillary effect of helping to harden the system against backscatter by limiting the FOV slightly; the narrower the bandwidth of the filter, the narrower is the FOV, and the less backscatter is collected.

After the PMT, the signal continues to a bias-tee circuit so we could separately monitor the DC and RF information from the detector. The DC information was viewed and recorded via a multimeter so that it could be compared to the amplitude information from the I/Q demodulator (which will be discussed shortly) as a check to help convince ourselves that our data made sense. The RF signal was then passed first through a 20dB amplifier, then a voltage controlled variable gain amplifier (VGA) with a gain of -50 to 50dB. We used this amplifier chain to raise the signal to a level acceptable to our demodulator.

C. RF Demodulator

We used an analog I/Q demodulator to determine the phase difference between a local oscillator (LO) reference signal, and the returned (RF) signal. From the demodulator we get In-Phase (I) and Quadrature-Phase (Q) data:

$$I = 0.125A_{LO}A_{RF} \cos(\varphi_{RF} - \varphi_{LO}) \quad (2)$$

$$Q = 0.125A_{LO}A_{RF} \sin(\varphi_{RF} - \varphi_{LO}) \quad (3)$$

where A_{LO} = amplitude of the reference signal
 A_{RF} = amplitude of the return signal
 φ_{LO} = phase of the reference signal
 φ_{RF} = phase of the return signal.

Using trigonometry, it can be demonstrated that the change in magnitude, ΔA , and the change in phase in degrees from the original signal, $\Delta\varphi$, can be computed:

$$\Delta A = \sqrt{I^2 + Q^2} \quad (4)$$

$$\Delta\varphi = \tan^{-1}\left(\frac{Q}{I}\right) \quad (5)$$

From this phase information, an absolute measurement of distance to target can be made by relating the change in phase to a real distance. The received phase of the RF signal changes in reference to the LO signal because of the time delay as the signal propagates to and from the target. Thus, if the target is farther from the receiver, the delay will be greater, so the phase difference between the received RF and sent LO signals will be greater. Note that because the signal must propagate both to and from the target, the computed distance will be twice that of the distance to the target. Hence, the distance R to the target can be found by:

$$2R = \frac{\Delta\varphi \cdot \lambda_{RF}}{360} = \frac{\Delta\varphi \cdot c}{360nf_{RF}} \quad (6)$$

where: c = the speed of light in vacuum
 $n \cong 1.33$, water's index of refraction
 λ_{RF} or f_{RF} = modulation wavelength or frequency.

The LO signal into the demodulator, as aforementioned, is fed from the same RF generator modulating the laser.

The demodulator provides the sum and difference of the incoming RF and LO signals, so low pass filters (LPF) must be used on the outputs to strip off the un-needed sum term. When selecting the bandwidth of these filters, one must keep in mind that a lower bandwidth means less noise on the outputs, but it also will limit the frequency at which one can sample to twice that of the filter bandwidth. We wish to eventually sample at 1MHz, so we used 500kHz filters.

C. Choice of Modulation Frequency (RF)

In general, modulating faster enables more accuracy in range measurements, as the phase can be better resolved. Consider, for example, a wavelength of 226m in water, or $f_{RF} \cong 1\text{MHz}$. Plugging this into (6), along with a phase difference of one degree, we get a distance of about 31cm. This means that for every degree difference in phase between the RF and LO signals that is measured, there is a 31cm change in calculated range. So, to get centimeter accuracy in an ideal distance measurement, one must be able to resolve $\frac{1}{31}$ of a degree phase change reliably, which leaves very little room for noise and other error in the system.

Now, compare this with a wavelength of 2.26m in water, or $f_{RF} \cong 100\text{MHz}$. Again plugging into (6), we see that now a difference of one degree translates to only about $\frac{1}{3}$ cm of calculated range difference. This means one need only be able to resolve three

degrees of phase difference to get centimeter accuracy in distance. The benefits of modulating faster are immediately apparent; such a system is much more robust against noise and measurement error.

However, there is an upper limit to modulation frequency, determined by the “unambiguous range,” the maximum distance in which a phase measurement can be regarded as meaningful (i.e. $\Delta\phi \leq 360^\circ$). As discussed before, we used a modulation frequency of 66MHz for the NIR laser, and 70MHz for the red and green. This translates to an unambiguous range of 1.71m and 1.61m in water, respectively. We felt this would give us enough accuracy, and we would be able to measure our entire desired range within the unambiguous range.

D. Controlling Dynamic Range

One of the major challenges we faced when designing and implementing our system was the large dynamic range of the optical signal amplitude. Since water, as discussed before, will attenuate optical signals exponentially and geometrically, a relatively strong signal must be used to be able to range a respectable distance. This means, unfortunately, that at short ranges the return amplitude will be relatively much larger, by two to four orders of magnitude or more, than the amplitude at longer ranges; the detector and the demodulator cannot handle this sort of dynamic range.

In order to compensate, we built a number of mechanisms into our system design, as can be seen in Fig. 3. To stay within the dynamic range of the demodulator, the VGA was used. We also adjusted the optical power into the tank to ensure that we stayed within the dynamic range of the PMT.

Another option would have been to alter the gain of the PMT. This is done by increasing the reverse bias on the tube, which has the effect of increasing the output current for a given amount of light incident on the detector. We did not use this control, however, and instead left it at a constant 90% of the maximum (to stay within the manufacturer recommended range) for the duration of our tests. By changing the reverse bias, we would have been changing the phase delay through the tube, thus altering our phase measurement, and ultimately the range to target calculation.

E. Calibrating the Overlap Function

While calibrating the overlap of source and receiver is not as important here as it was in the previous system, it can still affect the accuracy of the results. If the target is close or far enough away, the laser will illuminate a section of the target which may not be within the FOV of the detector (imagine if the FOV in Fig. 3 was narrower and did not intersect where the beam met the target). We calibrated the overlap by choosing a distance about half that of which we wanted to measure, and aimed the laser to be in the center of the detector’s FOV at that distance. This allowed the illuminated portion of the target to enter into the detector FOV quickly, and remain there for the length of the distance of interest.

F. Adjusting Water Turbidity

Turbidity of the tank water was varied using commercially available Maalox[®], a common practice in the underwater optics community. The active ingredients, aluminum hydroxide and magnesium hydroxide, are particles which scatter the light, but do little to alter the absorption properties of the water [12]. We chose to approximate the marine environments “coastal ocean” and “turbid harbor,” shown in Table I, as well as other turbidities; tap water, not salt water was used, as the difference between clean and salt water is negligible [1]. To more precisely model actual aquatic environments, absorption, too, would have to be altered. This could be done with dye, such as the organic black dye, Nigrosin.

IV. RESULTS

A. 830nm Near-IR

As the first test of our prototype system, we wanted to gather some baseline “best case” data in air, not through water. Since environmental effects and dynamic range were limited, we can expect this to be the best possible result with our system. Fig. 4 shows the performance of our 830nm prototype

TABLE I
PROPERTIES OF SELECTED WATER TYPES AT GREEN 532NM
(CONDENSED FROM [1]) (ALL IN m^{-1})

Water Type	Properties at Green		
	a	b	c
pure sea water	0.045	0.0025	0.043
clear ocean	0.114	0.037	0.151
coastal ocean	0.179	0.219	0.398
turbid harbor	0.366	1.824	2.19

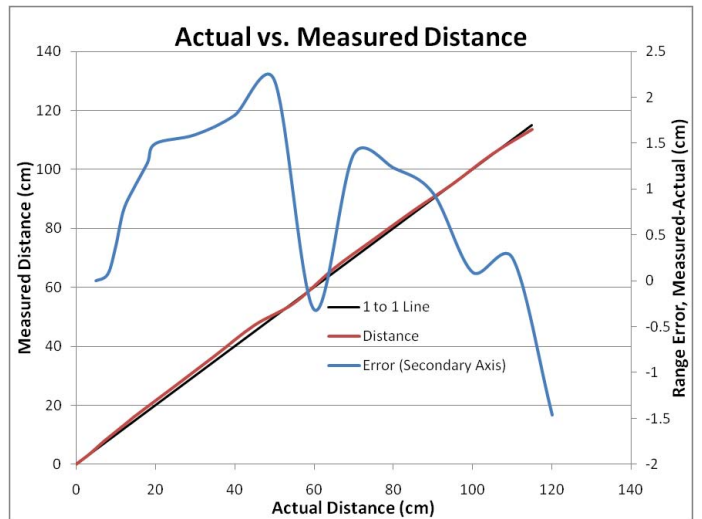


Fig. 4 Actual vs. Measured distance using our 830nm prototype system through air. Note that any deviation from the 1 to 1 Line is error, as shown by the blue line (secondary axis).

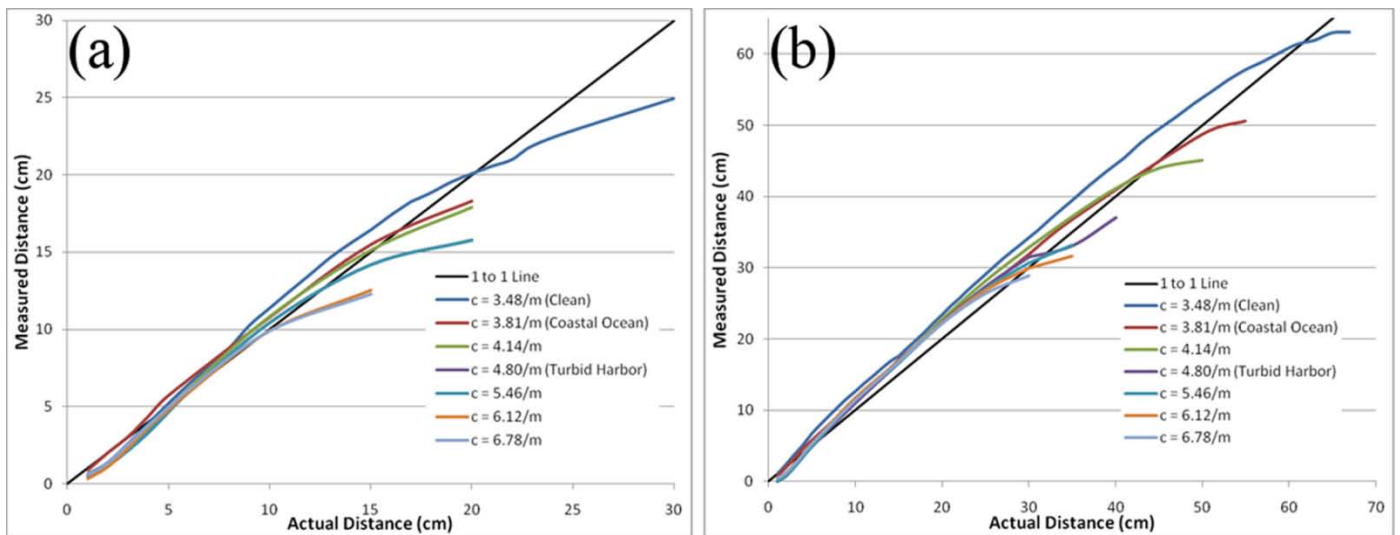
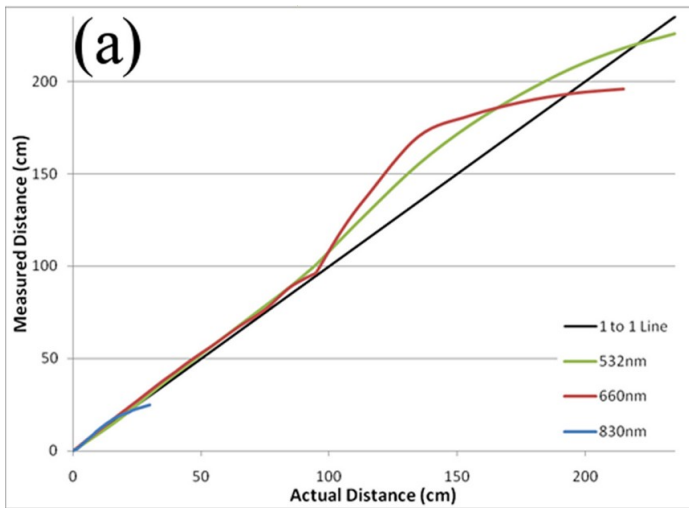


Fig. 5 Actual vs. Measured distance using our 830nm prototype system through water. (a) Weak target. (b) Strong target. Notice the increased ranging performance with a stronger, more reflective target.

in air. Actual distance and measured distance closely follow one another, as we expected; any deviation of this line from the “1 to 1 Line” ideal case is error. Note that the overlap function is very apparent in the error exhibited in the measurement- we aligned the laser to be in the center of the detector’s FOV at about 60cm, where the error dips to nearly zero.



Once the system was moved into the water tank, we were unable to range as accurately or as far as in air. Figs. 5a and 5b show a similar plot for both weak (black) and strong (grey) targets in water. Note the effect of a strong target- the return from the target is able to dominate the backscatter return for a greater distance, but eventually it too is backscatter limited. Also, as one might expect, more turbid water causes a degradation of system performance, leading to more error and less sensor range.

B. 660nm Red and 532 Green in Comparison

Having seen the effects of both beam attenuation due to turbidity and absorption, and of a strong or weak target, it is at this point most instructive to examine red and green wavelengths in comparison, using the NIR measurements as a baseline, as seen in Fig. 6. Since the worst case is typically the most useful in designing a system, a weak target will be

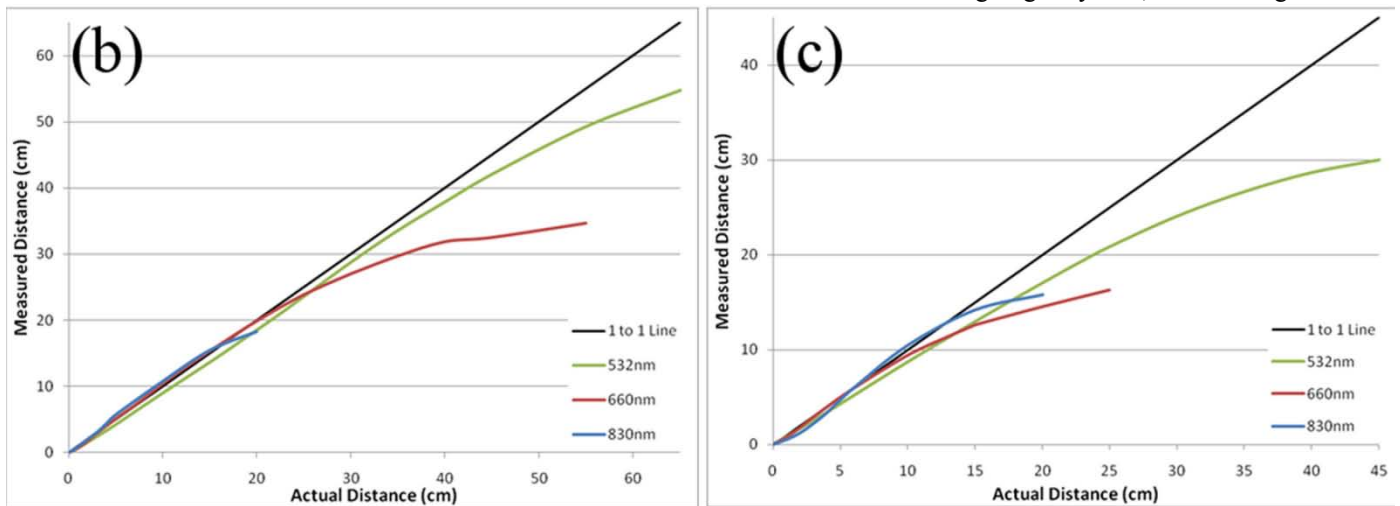


Fig. 6 Actual vs. Measured distance plots comparing all three of the wavelengths tested (black target). In clean water, the performance of lower wavelengths is much better, but as the water becomes more turbid, the performance converges. (a) Clean. (b) Coastal Ocean (c) Turbid Harbor.

considered when making the comparison. Fig. 6 shows Actual vs. Measured plots like those in Fig. 5, but instead shows all three wavelengths on one plot, separating plots by water turbidity. Selected turbidities include those for clean water (not pure), a coastal ocean area, and a turbid harbor.

In clean water, the shorter wavelengths vastly outperform the longer NIR. However, as the water begins to get more turbid, the different wavelengths' performance begins to converge. In fact, the NIR better maintains its performance characteristics over a range of turbidities compared to the green or red, just as predicted. This can be seen in Fig. 7, which shows clearly how the ability to range accurately converges for the red and NIR wavelengths as water turbidity increases; at first, the red is able keep under 3cm of error for a much longer distance than the NIR, but they soon converge in performance.

V. CONCLUSIONS AND FUTURE WORK

We applied the idea of a hybrid LIDAR-RADAR system to optical ranging in order to achieve centimeter-type range accuracy over the distance of meters with high range resolution. This would be a vast improvement over existing systems, optical or otherwise, at short ranges.

Using an optical wavelength in the NIR region helped to harden our system against the effects of changing turbidity levels of the water, but at the cost of not being able to range as far in clean water as we could with visible, especially blue-green, wavelengths. This is because NIR wavelengths absorb very quickly in even clean water, but are much less affected by scattering, the two components that make up total attenuation.

A modulation frequency of around 66MHz allowed us a theoretical maximum range measurement of about 1.71m within the unambiguous range, and afforded a one-half centimeter change in distance for every one degree of phase change. At 70MHz, the unambiguous range drops to 1.61cm.

Using the phase information of the modulation envelope, we were able to achieve centimeter-type accuracy, but we were only able to do this over a meter or more in ideal conditions, such as clean water with a strong target. The most accurate we can hope to be with this setup is demonstrated by our measurements in air. We were able to achieve less than 2.5cm of error over the entire measured range, 1.2m, in air. Even when limited by environmental effects, our system is still an improvement over the existing optical ranging system discussed earlier.

More work could be done to minimize the effects of the environment in limiting the range of the system. Also, dynamic range is still an issue. Three orders of magnitude or more need to be examined, depending on optical wavelength, which is impossible with a conventional detector. Techniques involving passive or mechanical apertures will be examined, as well as systems employing multiple lasers and detectors. Such a system could use one laser and receiver pair for near-field measurements, and another for far-field measurements. This would reduce the dynamic range requirement of each individual sensor, as well as allow the use of multiple wavelengths. Wavelengths which are absorbed less readily in water, for example, could be used for longer range measurements.

If a higher modulation frequency could be achieved, more accurate ranging information would be able to be gathered. However, this would come at the cost of a shorter unambiguous range, which is a drawback of the sinusoidal modulation (LIDAR-RADAR) scheme in this application.

A different scheme involving chaotic modulation techniques (CLIDAR) will be looked into in the future. Using chaotic waveforms to modulate an optical signal, we can take advantage of a very high bandwidth signal, as high as 15GHz, which is non-repeating [13]. This could have the potential for extremely accurate ranging which is not bounded by an unambiguous range.

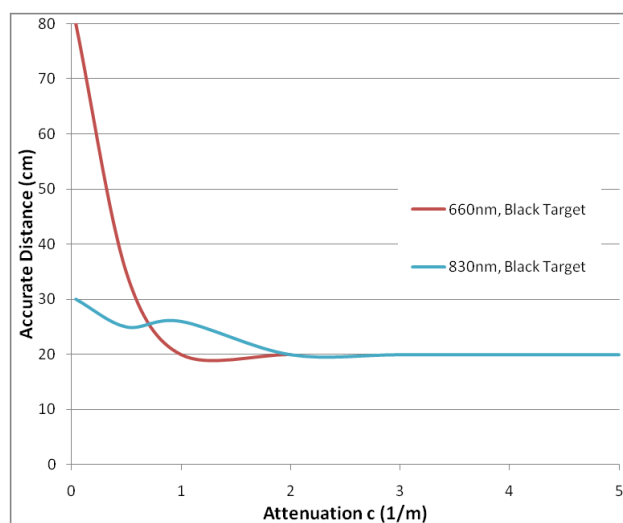


Fig. 7 The distance to which less than 3cm of ranging accuracy was maintained for NIR (830nm) and red (660nm) wavelengths for various water turbidities. (Here, attenuation is given at 532nm green as a reference.) The shorter wavelengths do better in clean water, but lose their advantage as the water gets more turbid.

REFERENCES

- [1] C D Mobley. (1994) The University of Maine In-situ Sound & Color Lab. [Online]. <http://miscslab.umeoce.maine.edu/education/Light&Water/D:/PAPER/>.
- [2] Paul J. Smith, "Optical Proximity Detector," 4,991,595, February 12, 1991.
- [3] L Mullen et al., "Amplitude Modulated Laser Imager," *Applied Optics*, vol. 43, pp. 3874-92, 2004.
- [4] Irvine and Pollack, "Infrared optical properties of water and ice spheres," *Icarus*, vol. 8, no. 1-3, pp. 324-360, 1968.

- [5] Buiteveld, Hakvoort, and Donze, "The optical properties of pure water," *SPIE Proceedings on Ocean Optics XII*, vol. 2258, pp. 174-183, 1994.
- [6] Moreal and Prieur, "Analysis of variations in ocean color," *Limnology and Oceanography*, vol. 22, pp. 709-722, 1977.
- [7] Palmer and Williams, "Optical properties of water in the near infrared," *Journal of the Optical Society of America*, vol. 64, pp. 1107- 1110, 1974.
- [8] Pope and Fry, "Absorption spectrum (380-700 nm) of pure water. II. Integrating cavity measurements," *Applied Optics*, vol. 36, pp. 8710-8723, 1997.
- [9] Smith and Baker, "Optical properties of the clearest natural waters (200-800 nm)," *Applied Optics*, vol. 22, pp. 177-184, 1981.
- [10] Shifrin, "Physical Optics of Ocean Water," *American Institute of Physics*, 1988.
- [11] Hamamatsu Photonics, Photosensor Modules H6779/H6780/H5784 Series, June 1999, Used module H6780-04.
- [12] Theodore J Petzold, "Volume scattering functions for selected ocean waters," University of California, San Diego, Scripps Institution of Oceanography, Visibility Laboratory, San Diego, SIO_72-78, 1972.
- [13] Fan-Yi Lin and Jia-Ming Liu, "Chaotic Lidar," *IEEE Journal of Selected Topics in Quantum Electronics*, vol. 10, no. 5, pp. 991-991, September/October 2004.